Annals of Work Exposures and Health, 2021, Vol. 65, No. 8, 966–978
doi: 10.1093/annweh/wxab011
Advance Access publication 27 July 2021
Original Article

Original Article

Characterizing the Chemical Profile of Incidental Ultrafine Particles for Toxicity Assessment Using an Aerosol Concentrator

M. Viana[1,*], A. Salmatonidis[1], S. Bezantakos[2], C. Ribalta[1], N. Moreno[1], P. Córdoba[1], F.R. Cassee[3], J. Boere[3], S. Fraga[4,5], J.P. Teixeira[4,5], M.J. Bessa[4,5] and E. Monfort[6]

[1]IDAEA-CSIC, Barcelona, Spain [2]Université du Littoral Côte d' 'Opale, Dunkerque, France [3]RIVM, Bilthoven, The Netherlands [4]Department of Environmental Health, National Institute of Health Dr Ricardo Jorge, Porto, Portugal [5]EPIUnit-Instituto de Saúde Pública, Universidade do Porto, Porto, Portugal [6]ITC, Castellón, Spain

* Author to whom correspondence should be addressed. E-mail: mar.viana@idaea.csic.es

Submitted 4 August 2020; revised 1 December 2020; editorial decision 18 January 2021; revised version accepted 28 January 2021.

Abstract

Incidental ultrafine particles (UFPs) constitute a key pollutant in industrial workplaces. However, characterizing their chemical properties for exposure and toxicity assessments still remains a challenge. In this work, the performance of an aerosol concentrator (Versatile Aerosol Concentration Enrichment System, VACES) was assessed to simultaneously sample UFPs on filter substrates (for chemical analysis) and as liquid suspensions (for toxicity assessment), in a high UFP concentration scenario. An industrial case study was selected where metal-containing UFPs were emitted during thermal spraying of ceramic coatings. Results evidenced the comparability of the VACES system with online monitors in terms of UFP particle mass (for concentrations up to 95 μg UFP/m^3) and between filters and liquid suspensions, in terms of particle composition (for concentrations up to 1000 μg/m^3). This supports the applicability of this tool for UFP collection in view of chemical and toxicological characterization for incidental UFPs. In the industrial setting evaluated, results showed that the spraying temperature was a driver of fractionation of metals between UF (<0.2 μm) and fine (0.2–2.5 μm) particles. Potentially health hazardous metals (Ni, Cr) were enriched in UFPs and depleted in the fine particle fraction. Metals vaporized at high temperatures and concentrated in the UF fraction through nucleation processes. Results evidenced the need to understand incidental particle formation mechanisms due to their direct implications on particle composition and, thus, exposure. It is advisable that personal exposure and subsequent risk assessments in occupational settings should include dedicated metrics to monitor UFPs (especially, incidental).

What's important about this paper

Our work addresses the challenge of characterizing the bulk chemical composition of ultrafine particles in occupational settings, for exposure and toxicity assessments. We tested the performance of an aerosol concentrator (VACES) to simultaneously sample ultrafine particles (UFPs) on filter substrates and as liquid suspensions, in a high UFP concentration scenario. An industrial case study was selected where metal-bearing UFPs were emitted. We report the chemical exposures characterized in the industrial facility, and evidence the comparability of the VACES system with online monitors for UFP particle mass (up to 95 µg UFP/m^3) as well as between UFP chemical composition on filters and in suspension. This supports the applicability of this tool for UFP collection in view of chemical and toxicological characterization of exposures to incidental UFPs in workplace settings.

Graphical Abstract

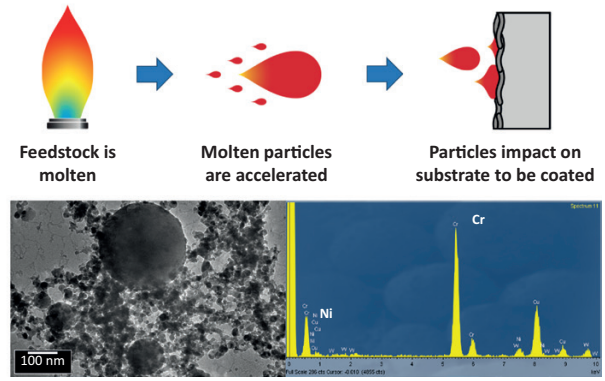

Keywords: morphology; new particle formation; metal nanoparticles; nanoparticles; occupational; versatile aerosol concentrator; workplace

Highlights

- The VACES system is a useful tool for UFP sampling in high-concentration settings.
- UFP collected simultaneously on filters and in suspension showed good comparability.
- UFP chemical profiles were characterized.
- Health-hazardous metals Ni and Cr accumulated in UFPs.
- Understanding emission mechanisms is key to identifying exposure sources.

Introduction

While the adverse health effects and burden of exposure to coarse and fine atmospheric particles are described in detail in the literature (Lelieveld *et al.*, 2015; Cohen *et al.*, 2017; Burnett *et al.*, 2018; Pope et al., 2019; among others), significant gaps still remain regarding nanoparticles (NPs) and ultrafine particles (UFPs, <100 nm) despite their ability to penetrate deeper in the respiratory tract (Oberdörster, 2001; Oberdörster *et al.*, 2007). UFPs are a key pollutant in urban and industrial areas, in occupational and ambient air, resulting from anthropogenic sources such as internal combustion engines and other sources of thermo-degradation (Terzano *et al.*, 2010; Morawska *et al.*, 2017).

In occupational industrial settings, efforts to evaluate environmental health and safety implications of UFP are frequently based on physical particle properties such as particle number concentration or size distribution (Gonzalez-Pech *et al.*, 2019; Oberbek *et al.*, 2019; among

others). When referring to engineered nanomaterials (ENMs), the body of literature reporting physical properties is large (Maynard *et al.*, 2004; Maynard and Aitken, 2007; Hämeri *et al.*, 2009; Kuhlbusch *et al.*, 2011; Brouwer *et al.*, 2012; Hristozov *et al.*, 2012; Falk *et al.*, 2016; among many others). However, chemical properties (e.g. metal content) and sources are also determinants of health risks (Perrone *et al.*, 2010; Billet *et al.*, 2018; Shao *et al.*, 2018; Gerlofs-Nijland *et al.*, 2019). Literature on workplace UFP chemical composition is currently relatively scarce (Ntziachristos *et al.*, 2007; Terzano *et al.*, 2010; Viana et al., 2015, 2014; Corsini *et al.*, 2017; Ozgen *et al.*, 2017; Mendes *et al.*, 2018; Gonzalez-Pech *et al.*, 2019), one of the reasons being that it is frequently difficult to obtain enough released material for a proper characterization and more so for toxicological testing (Kuhlbusch *et al.*, 2018). As a result, the characterization of bulk UFP chemical composition for exposure and toxicity assessments still remains a challenge, evidenced by an increasing interest in assessing the concentrations and physico-chemical properties of incidental UFPs in workplaces (Curwin and Bertke, 2011; Stone *et al.*, 2017; Viitanen *et al.*, 2017; Gonzalez-Pech *et al.*, 2019; Keyter *et al.*, 2019).

The present work aimed to assess the applicability of a Versatile Aerosol Concentration Enrichment System (VACES; Kim *et al.*, 2001; Geller *et al.*, 2002; Freney *et al.*, 2006; Liu *et al.*, 2019) for collection of airborne UFPs in occupational settings, in view of UFP toxicity assessment (reported elsewhere, Bessa *et al.*, 2021). The case study selected was a thermal spraying facility where two different types of technologies were used to spray ceramic coatings (Salmatonidis *et al.*, 2019a), in the framework of SIINN-ERANET project CERASAFE (Safe Production and Use of Nanomaterials in the Ceramic Industry). Advanced ceramic materials and processing technologies have a strong potential for incidental formation and release of UFP into workplace air (Fonseca *et al.*, 2015; Viana *et al.*, 2017; Ribalta *et al.*, 2019b; Salmatonidis et al., 2019a, 2019b; Bessa *et al.*, 2020). The use of the VACES system provided a unique opportunity to collect particles, simultaneously, on filter substrates for chemical characterization and as suspensions for toxicity assessments (discussed elsewhere; Bessa *et al.*, 2021). The target analyses (in this case, toxicity and chemical characterization) determine the need for different sample preparations (Stone *et al.*, 2017). In addition to testing the applicability of the tool, our work aimed to generate new information on the chemical composition of incidental metallic UFPs, as well as of fine ($PM_{2.5}$) and coarse ($PM_{2.5–10}$) aerosols, emitted during plasma spraying of ceramic materials onto metal substrates. The results obtained contribute to the growing body of literature on chemical profiling of occupational exposures to incidental UFPs, specifically of metal-containing UFPs, and provide the basis for toxicity and subsequent risk assessment of the particles emitted during this kind of industrial activity. Studies on exposure to incidental UFP in occupational settings are paramount for the design of effective health and safety protocols, which should include incidental UFPs as a key potential health risk.

Materials and methods

Site description

Measurements were carried out at an industrial-scale metallurgy workshop (T.M. Comas) in the vicinity of Barcelona (Spain), in November 2017. Particle emissions were monitored during spraying of ceramic powders onto metal surfaces to produce thermal-resistant coatings (Ribalta *et al.*, 2019a; Salmatonidis *et al.*, 2019a). The spraying activities were representative of the usual operating conditions in the plant, which were concurrent to other activities (welding, laser cladding, among others) in nearby sections of the plant. The layout of the spraying facilities is described in Fig. 1: three spraying booths were located in an area of approximately 240 m^2 (14 m wide × 17 m in length), including a central area for worker transit (referred to as the worker area). The operators worked both inside and outside the booths during spraying. The booth doors were frequently open while spraying due to the need to introduce new pieces to be coated. Workers wore personal protective equipment (FFP3 masks) inside the booths but removed them every time they stepped in the worker area. As a result, they were exposed to particles originating inside the booths and to those transported and formed in the worker area.

The operational characteristics of each of the spraying activities and booths are reported elsewhere (Ribalta *et al.*, 2019b; Salmatonidis *et al.*, 2019a). The main difference between booths #1 and #3, relevant for this work, are:

- Booth #1: high spraying temperatures (5–20 × 10^3°C) and low spraying velocities (200–500 m/s). Spraying technique: atmospheric plasma spraying (APS).
- Booth #3: high spraying velocities (425–1500 m/s) and lower temperatures (2.9 × 10^3°C). Spraying technique: high velocity oxy fuel (HVOF).

Ultrafine particle sampling, characterization and monitoring

A VACES (Kim *et al.*, 2001; Geller *et al.*, 2002; Liu *et al.*, 2019) was used to collect aerosols in three size fractions: coarse ($PM_{2.5–10}$), fine + UF ($PM_{2.5}$) and quasi-UF

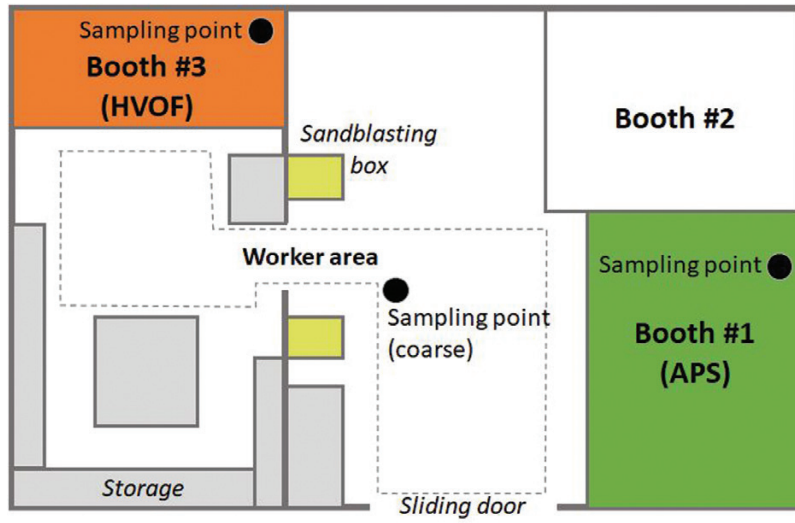

Figure 1. Schematic representation of the thermal spraying facility.

(<0.2 µm; referred to as UF in this manuscript) particles. The fine particle mass concentrations were calculated indirectly by subtraction of the UF from the fine + UF size fraction. In short, a single-nozzle virtual impactor collects the coarse fraction, whereas the fine fraction is collected by drawing air samples through two parallel lines. The fine size fractions go through a saturation–condensation system, which grows particles to 2–3 µm droplets, and then concentrate them by virtual impaction (Liu *et al.*, 2019). The VACES system has been validated for ambient aerosol (Kim *et al.*, 2001; Ning *et al.*, 2006; Ntziachristos *et al.*, 2007) and at (relatively low) UFP mass concentrations (e.g. 2.7 µg/m^3; Ntziachristos *et al.*, 2007). The present work presents an application in indoor air and for high UFP concentrations (up to 95 µg/m^3; see Section 3.1).

The VACES enriches ambient particles by a factor of 20–40, depending on the output flow rate required (Ntziachristos *et al.*, 2007). In the present study, the VACES operated at 110 l/min, resulting in a concentration enrichment factor of 31. The experimental enrichment factor of the VACES is similar to what theoretically expected, based on its operating flows, for all particles sizing above 50 nm, irrespective of whether they are hydrophobic or not (Kim *et al.*, 2001). Time-integrated aerosol samples were collected over 8-hr shifts from indoor air: fine and UF particles were collected directly from inside the spraying booths, and the coarse fraction was sampled from the worker area given that no primary coarse particle emissions were expected to be generated inside the booths. Even if particle agglomeration were considered due to the high particle number emissions, this was not expected to result in coarse mode particles inside the booths. Particle samples were collected simultaneously on Teflon filters for elemental analysis and gravimetric determination. and in a BioSampler (SKC Inc.) using de-ionized water (the sample flowing directly through the liquid) for toxicity testing (Bessa *et al.*, 2021). Additional sets of Teflon filters were placed after the BioSamplers to collect aerosols potentially not retained in the sampler due to lower sampling efficiency linked to particle size and/or composition. Particle losses in the biosamplers ranged between 1.8 and 4.6%, lower than the usual 5%. In total, 18 filter samples (8-h) were collected: 6 from booth #1 (three collecting the concentrated aerosol flow and three downstream of the BioSampler), and 12 from booth #3 (same as in booth #1, on two different days). The complexity of the VACES instrument and the need to minimize any interference with the plant's production process limited the collection of a larger number of samples, as is usual in occupational real-world studies. However, the industrial production monitored is typically repetitive and the samples collected are considered fully representative of the 8-hr shifts. Based on the limited data availability, the comparisons between different cases (e.g. booths, Figs. 2, 3 and 6) should be considered descriptive and not based on statistical analyses.

Particle mass concentrations were determined on the Teflon filters after conditioning at constant temperature and relative humidity by gravimetry (microbalance XP105DR Mettler Toledo; sensitivity ±10 µg). Filters were then acid digested (5 ml HF, 2.5 ml HNO_3, 2.5 ml $HClO_4$) according to Querol *et al.* (2001) and the

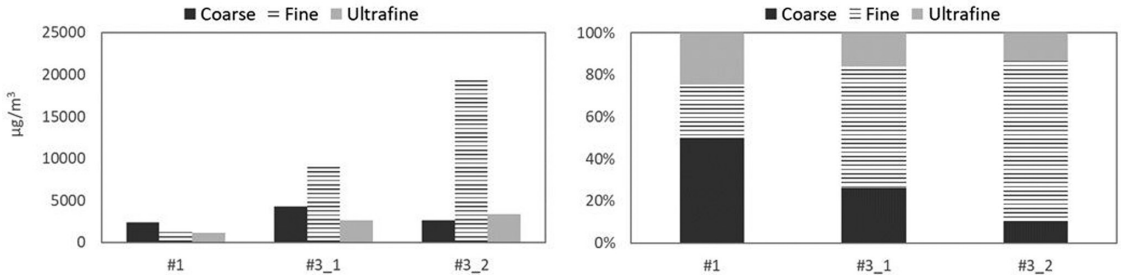

Figure 2. Absolute and relative particle mass contributions from the size fractions measured (coarse, fine and UF) to the total aerosol mass. Concentrations reported in the y-axis as measured (concentrated, by a factor of 31; µg/m³). The x-axis shows the three 8-h aerosol samples collected (sample #1 during APS spraying in booth #1, and samples #3_1 and #3_2 during HVOF spraying in booth #3 on two different days).

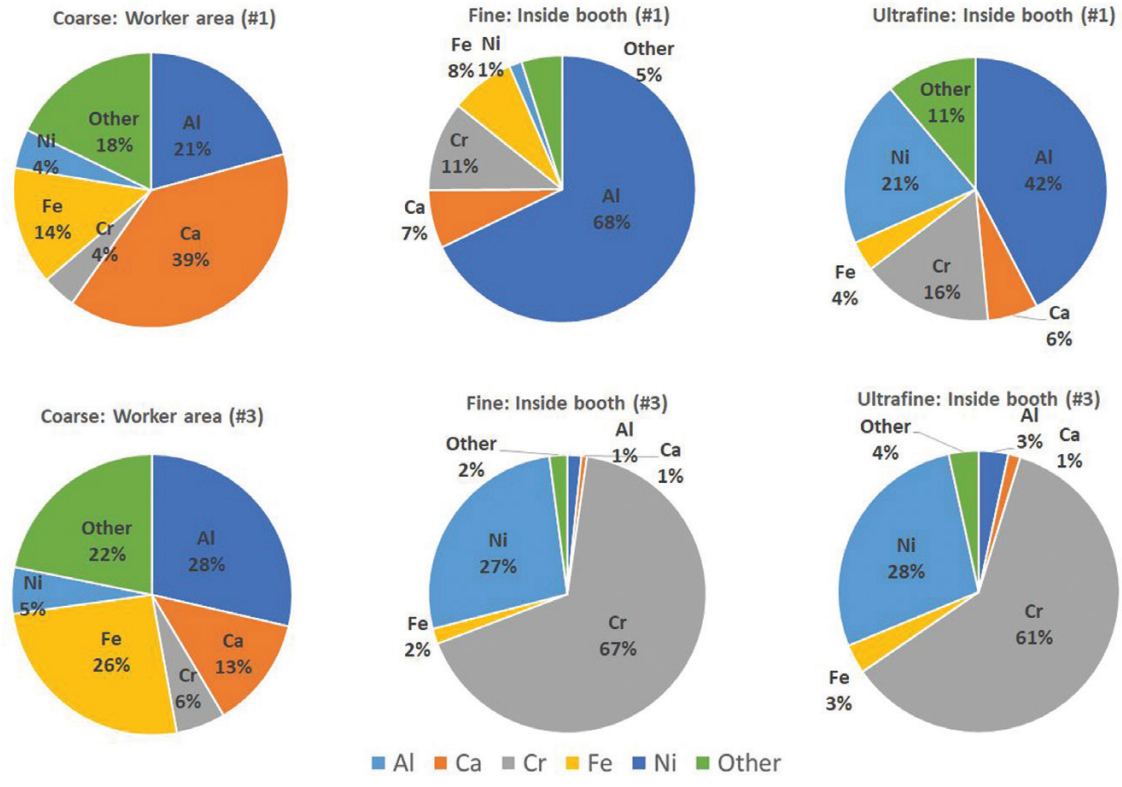

Figure 3. Size-resolved chemical composition (in %) of coarse, fine and UF particles in the worker area and inside the spraying booths.

extracts analysed by Inductively Coupled Plasma Mass Spectrometry (ICP-MS) and Inductively Couple Plasma Optical Emission Spectrometry (ICP-OES). The elemental composition was also determined directly on the Teflon filters by Energy Dispersive X-Ray Fluorescence Spectrometer (EDXRF). Three different analytical techniques were used for quality-control purposes. The elements determined were Li, Ti, V, Cr, Mn, Co, Ni, Cu, Zn, As, Se, Rb, Sr, Y, Zr, Nb, Mo, Cd, Sn, Sb, Cs, Ba, La, Ce, W, Tl and Pb. Finally, particle morphology was characterized by Transmission Electron Microscopy (TEM) at the Barcelona University.

In parallel to particle collection, particle mass, number concentrations and size distributions were recorded continuously with a NanoScan-SMPS (Nanoscan SMPS Nanoparticle Sizer 3910, TSI Inc. USA; 10–420 nm; 60-s

time resolution) and a MiniWRAS aerosol spectrometer (Mini Wide Range Aerosol Spectrometer model 1371, GRIMM Aerosol Technik Ainring GmbH & Co.; 10 nm to 35 µm; 6-s time resolution). The results from the online measurements carried out in the plant are reported elsewhere (Ribalta *et al.*, 2019b; Salmatonidis *et al.*, 2019a).

Feedstock characterization

A portion of the raw feedstock materials was acid-digested in duplicate by using a two-step digestion method devised by Querol *et al.* (2001) to retain volatile elements. This consisted of weighing ca. 0.1 g powdered sample into a PFTE vial and adding Primar grade concentrated HNO_3 to pre-digest the organic fraction. This was followed by addition of concentrated Primar grade HF: HNO_3:$HClO_4$ mixture and evaporation on a hot plate at 240°C, the purpose being digestion of mineral phases. The concentrations of major elements in the acid digests were determined using Inductively Coupled Plasma Atomic-Emission Spectrometry (ICP-AES, Iris advantage Radial ER/S device from Thermo Jarrell-Ash). Trace elements were analysed by Inductively Coupled Plasma Mass Spectrometry (ICP-MS, X-SERIES II Thermo Fisher Scientific, Bremen, Germany), operating the instrument with a collision cell to remove spectral interferences and using 10 µg L-1 In as internal standard.

Results and discussion

Particle mass and number concentrations

Size-resolved particle mass concentrations sampled with the aerosol concentrator are reported in Fig. 2, for the three 8-h aerosol samples collected (sample #1 during APS spraying in booth #1, and samples #3_1 and #3_2 during HVOF spraying in booth #3 on two different days). High particle mass concentrations were collected, with the fine fraction reaching up to 19 mg/m^3 (sample #3_2) while the highest UF mass concentration was 3 mg/m^3 (#3_2) and the highest coarse concentration, 4 mg/m^3 (#3_1) (Fig. 2, left). Assuming an aerosol concentration factor of 31 as reported by Kim *et al.* (2001), this would result in mean 8-h concentrations of up to 95, 600 and 130 µg/m^3 for the UF, fine and coarse fractions, respectively. These concentrations are higher yet comparable to those reported e.g. during welding (a foundry and a machining centre; 37–54 µg UFP/m^3; Gonzalez-Pech *et al.*, 2019). As shown in Fig. 2 (right), the coarse fraction was highest in relative terms in the worker area when spraying was active in booth #1 while the fine fraction was clearly dominant during spraying inside booth #3. Despite this, the high UF mass concentrations measured should be highlighted (95 µg/m^3 as 8-h mean), especially due to their metal content (described below). The mean mass concentrations measured are comparable to concentrations monitored with online instruments during the same activity in other periods of time (PM_1 between 61 µg m^3 booth #1 and 640 µg m^3 in booth #3; Salmatonidis *et al.*, 2019a), which confirms the representativeness of the aerosol samples collected and the validity of the VACES system (in terms of mass concentrations) for high exposure scenarios. The larger contribution of coarse particles in the worker area during spraying in booth #1, compared to those from booth #3, is consistent with the major particle emission

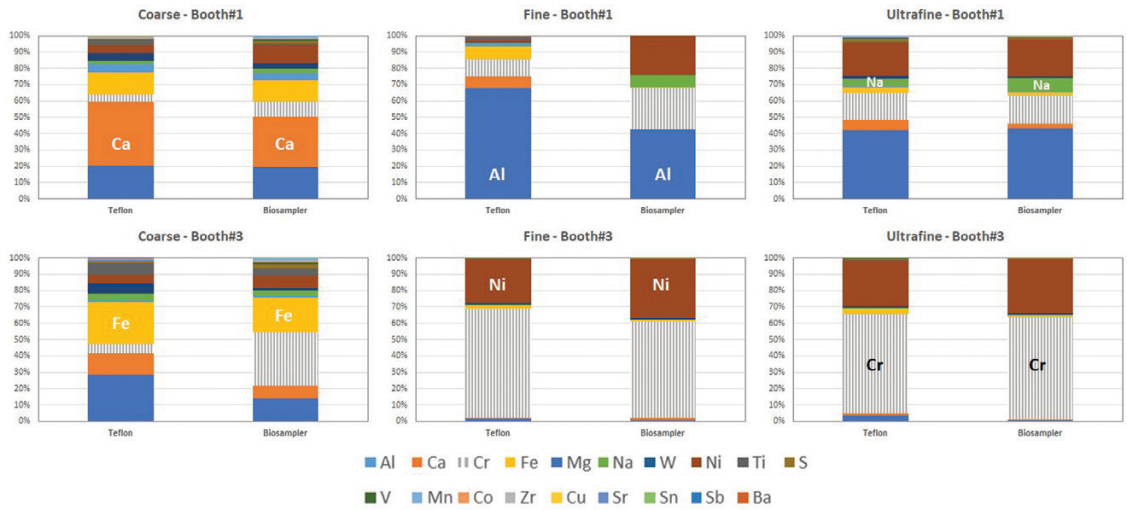

Figure 6. Relative chemical composition of coarse, fine and UF particles collected on Teflon filter substrates and in the biosamplers. Key elements are highlighted to facilitate reading.

Table 1. Element concentrations (in µg/m³) in coarse, fine and UF particles emitted from booths #1 and #3. The fine fraction was calculated indirectly from the fine + UF and UF fractions. Aerosol concentration factor: 31.

Fraction	Coarse	Coarse	Fine + UF	Fine + UF	Fine	Fine	UF	UF
Booth	#1	#3	#1	#3	#1	#3	#1	#3
Feedstock	Al/Ti/Cr/Ni	Ni/Cr/Co/W	Al/Ti/Cr/Ni	Ni/Cr/Co/W	Al/Ti/Cr/Ni	Ni/Cr/Co/W	Al/Ti/Cr/Ni	Ni/Cr/Co/W
Al	139	252	379	133	232	93	147	40
Ca	260	113	45	52	24	36	22	16
Cr	27	50	93	4534	37	3825	56	709
Fe	93	226	39	141	27	102	13	39
Mg	34	14	9.1	7.0	5.5	4.7	3.7	2.3
Na	12	35	16	21	1.6	15	15	5
W	33	54	8.4	73	2.5	58	5.9	14
Ni	31	47	76	1864	5.3	1539	71	325
Ti	16	63	7	32	5	24	2	8
S	5.6	6.9	4.8	6.9		2.1	7.5	4.8
V	0.20	0.40	0.08	0.80	0.05	0.66	0.03	0.14
Mn	1.9	2.9	2.2	3.3	0.69	2.22	1.5	1.1
Co	4.2	4.9	1.4	8.7	0.3	7.4	1.1	1.4
Zr	4.0	5.4	1.1	1.8	0.56	1.25	0.49	0.54
Cu	1.9	2.0	0.7	1.5	0.25	0.84	0.40	0.66
Sr	0.41	0.38	0.09	0.17	0.07	0.13	0.03	0.04
Sn	3.2	2.5	1.9	2.2	0.01	0.71	1.9	1.5
Sb	0.4	0.3	0.2	0.3	<0.01	0.08	0.3	0.2
Ba	1.2	1.1	0.3	0.41	<0.01	<0.01	0.01	<0.01
Sum	*668*	*882*	*686*	*6883*	*341*	*5713*	*348*	*1169*
Mass	*2377*	*3446*	*2378*	*17328*	*1213*	*14344*	*1165*	*2985*
% det.	*28%*	*26%*	*29%*	*40%*	*28%*	*40%*	*30%*	*39%*

mechanisms (hypersonic impaction *vs*. melting/fusion of the feedstock material; Salmatonidis *et al*., 2019a).

Chemical composition of the concentrated aerosol

Size-resolved particle chemical composition (in μg/m^3), determined by ICP-MS and ICP-OES, is presented in Fig. 3 and Table 1 (mean results for both sampling days are presented for booth #3). The elemental composition was also determined by XFR for quality-control purposes. The inter-comparison between both analytical methods provided good results for the majority of the elements analysed, with especially high intra-method correlations for Ca, Fe, Ti, Cr, Sr, Co, Ni, W, Zn and Pb ($R^2 > 0.98$; Fig. S1 in Supporting Information), which include the main tracers of the feedstock materials sprayed (Table S1 in Supporting Information). Based on this quality control, for the following analyses the data obtained by ICP-MS and ICP-OES were used. The elemental composition analysed accounted for 26–40% of the aerosol mass determined by gravimetry (Table 1), with carbonaceous species (elemental and organic carbon), secondary inorganic species (SO_4^{2-}, NO_3^-, NH_4^+) and water accounting for the remaining aerosol mass.

Different results were obtained for the coarse fraction, on the one hand, and the fine and UF fractions, on the other (Fig. 3). UF particle composition was dominated by the elemental composition of the feedstock: in booth #1 (feedstocks ANVAL 50/50, Cr/Ni and Amdry 6228, Al_2O_3+TiO_2), major contributions were detected from Al (147 μg/m^3; Table 1), Cr (56 μg/m^3) and Ni (71 μg/m^3); while in booth #3 (feedstock Woka 3702-1, WC, CrC, Ni, Co) the dominant elements were Cr (709 μg/m^3) and Ni (325 μg/m^3). Once again, the high mass concentrations of potentially health-hazardous metals measured in UFPs should be highlighted as an exposure risk in this occupational setting. The composition of the feedstock materials was obtained from the product technical specification sheets (Table S1) and from direct quantification in the laboratory (Table S2). Contributions were also detected from S to the UF fraction, which were low in comparison to other elements but high in absolute terms (4.8–7.5 μg/m^3).

The chemical composition of the fine and UF fractions was highly similar during spraying in booth #3, whereas significant differences between both size fractions were observed for aerosols generated inside booth #1. In booth #1, UF particles were made up by 42% of Al, 20% of Ni and 16% of Cr, as expected based on the feedstock powders composition (Table S1). Conversely, fine particles (0.2–0.25 μm) were strongly enriched in Al (68%) and depleted in Cr (from 56 μg/m^3 to 37 μg/m^3 in UF and fine particles, respectively) and Ni (from 71 μg/m^3 in UF to 5 μg/m^3 in fine particles), in comparison to UFPs. The reason for this different size-resolved composition could be the spraying temperature: spraying in booth #1 is characterized by high temperatures at the nozzle (5–20×10^3°C), which are above the vaporization temperatures of both Ni (2800°C) and Cr (2650°C). Therefore, Ni and Cr probably volatilized during spraying in booth#1. After volatilization, the presence of Ni and Cr in UF particles could be explained as resulting from new particle formation due to condensation of the gaseous components (Byeon *et al*., 2008), which would also explain the low concentration of these elements in fine particles. UF particle agglomerates formed by spherical Cr/Ni particles (<20 nm primary particle size; Fig. 4a) support this hypothesis. This would not be the case for booth #3, where spraying temperatures were lower at the nozzle (2.9 × 10^3°C). Thus, it may be concluded that the metal content (and potential toxicity) of the UF size fraction in booth#1 was enhanced by the spraying temperature, which was not the case in booth #3. These results highlight the relevance of understanding the specifics of the particle formation mechanisms of incidental particles, as these have major and direct implications on particle composition and, thus, exposure.

Aside from this new-particle formation mechanism, UF particles containing Ni and Cr were released in both booths through fugitive emissions during handling of the feedstock powders and/or through hypersonic impaction on the surface being coated (as reported in Salmatonidis *et al*., 2019a), which resulted in irregular-shaped particles. These were observed during spraying in booth #3 (with lower spraying temperatures, Fig. 4b) but also in booth #1 (Fig. 4c).

The case of Al requires further research: while it vaporized during spraying in booth #1 (vaporization temperature = 2327°C) and was detected forming spherical UF particles together with Ni and Cr (Fig. 4a), it was also detected as the major component in spherical particles in the fine mode (Fig. 4d). As a result, higher Al concentrations were measured in fine particles when compared to the UF mode (Fig. 3), in contrast to what was observed for Ni and Cr. Possible explanations for this behaviour could be different growth rates of Al particles when compared to Ni-Cr particles, or that Al particles formed after vaporization had a larger formation diameter than Ni-Cr ones, which would subsequently have grown by coagulation. Further research is necessary to understand this process.

Finally, the impact of particle emissions in the worker area was also evident for coarse particles, which showed similar average chemical characteristics during spraying

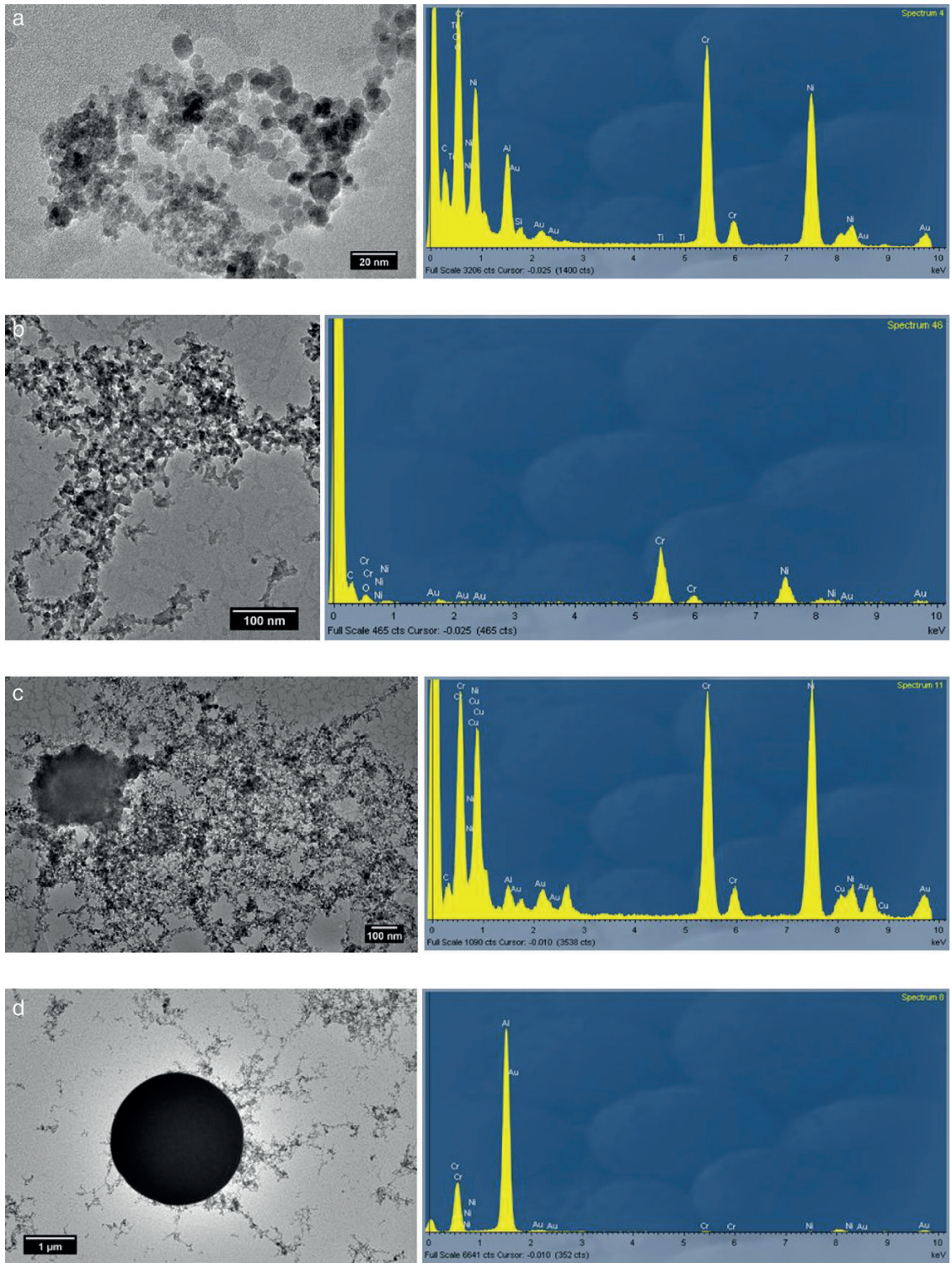

Figure 4. TEM-EDX images showing (a) spherical Cr/Ni/Al UF particles collected in booth #1; (b) irregular Cr/Ni UF particles from booth #3; (c) irregular Cr/Ni UF particles from booth #1; (d) spherical Al fine particle from booth #1.

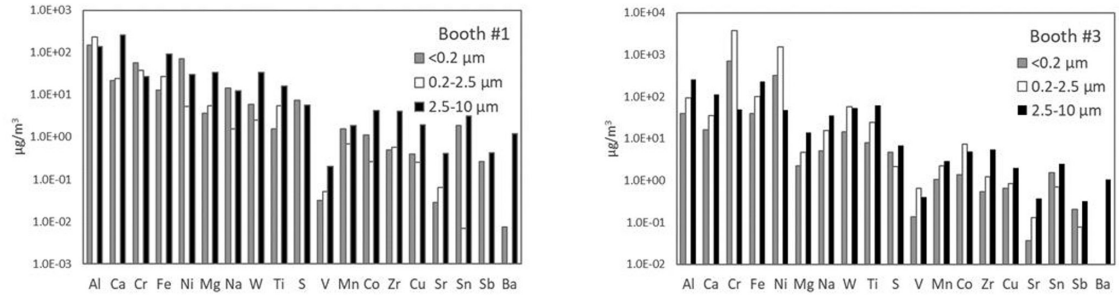

Figure 5. Distribution of the element concentrations across the three different size fractions collected (concentrated, by a factor of 31).

from both booths. Short-term impacts on coarse particle mass from the different booths were also detected, using online instrumentation (Salmatonidis *et al.*, 2019a). The main components of the coarse fraction were Al (139–252 µg/m³), Ca (113–260 µg/m³) and Fe (93–226 µg/m³), followed by S (5.6–6.9 µg/m³), Co (4.2–4.9 µg/m³), Zr (4.0–5.4 µg/m³) and Sb (0.3–0.4 µg/m³) (Fig. 3, Table 1). These tracers are not representative of the feedstock materials sprayed (with the exception of Al in booth #1), and they include markers of urban background emissions (e.g. Sb) in similar concentrations to other urban environments (Sb = 9–12 ng/m³ before aerosol concentration, versus 11 ng/m³ in urban background sites in Spain; Querol *et al.*, 2004). Thus, the chemical composition of the coarse fraction reflects the indoor background aerosol mix, influenced by outdoor infiltration (ambient air) and indoor air by emissions from diverse stages of metal processing activities in the workshop such as welding, polishing, laser processing, metal grinding, and plasma spraying, among others.

Element size distribution

Fig. 5 shows the distribution of element mass concentrations in the three size fractions collected (concentrated), during spraying in both booths. Once again, different behaviours were observed for the different types of aerosols. Based on Fig. 2, the size distribution of the aerosol mass from booth #1 was dominated by coarse particles (50% of the mass) and, as shown in Fig. 5, this aerosol mass was mainly driven by Ca, Al and Fe (260, 139 and 93 µg/m³, respectively). However, while Ca and Fe showed a coarse size distribution (Fig. 5), in the case of Al larger contributions were measured from fine and UF particles (232 and 147 µg/m³, respectively) than from coarse particles. The same was true for Ni and Cr, determined mostly in UF particles (71 and 56 µg/m³, respectively), but not for Ti (mainly coarse). Thus, for Al, Ni and Cr, the spraying activity generated fine and UF particles from the feedstock either through volatilization of the powder and subsequent new particle formation and growth, or via primary emission during impaction of the feedstock on the surfaces to be coated (Fig. 4). Ti did not follow the same size distribution pattern, possibly due to its higher vaporization temperature (3260°C), and was thus mainly found in coarse particles (mean aggregate diameter of the feedstocks = 35–77 µm according to the technical specification sheets, Table S1).

On the other hand, elements not present in the feedstock (e.g. Ca, Fe) were mostly detected as coarse particles, probably emitted by simultaneous sources in the facility. Other elements found mainly in coarse particles and originating from cross-contamination and background aerosols were Mg, W, Co, Zr, Cu, Sn and Ba.

During spraying in booth #3 (lower temperatures and higher speeds) the majority of the elements (Al, Ca, Fe, Mg, Na, W, Ti, S, Zr, Cu, Sr, Sn, Sb, Ba) showed a dominantly coarse size distribution. However, the high Ni and Cr mass concentrations determined in fine and UF particles (Cr = 3825 µg/m³ in fine and 709 µg/m³ in UF particles; Ni = 1539 and 325 µg/m³, respectively) drove the overall aerosol mass size distribution towards the finer size fractions, as shown in Fig. 2. Fine and UF particles were probably generated from the initial powder (mean diameter of aggregates = 29.2–34.3 µm, Table S1) by direct emission during spraying (Fig. 4b), given the lower spraying temperatures applied in this booth. The dominant particle emission mechanism at lower temperatures was mechanical impaction of the feedstock onto the material being coated, which resulted in UF and fine particles (Salmatonidis *et al.*, 2019a).

As a result, it may be concluded that in the case of booth #3 the chemical composition and size distribution of the particles emitted were mainly determined by the feedstock material, while in the case of booth #1 the relative contribution from indoor background aerosols was higher. The different size distribution patterns observed for the different types of particles sampled are

thus dependent on spraying conditions (e.g. temperature, speed, duration) and also on environmental conditions (influence of indoor background particles), which in turn impact exposure.

Comparison between filter and biosampler particle composition

The aerosol concentrator uses Teflon filters downstream of the VACES and in parallel to the Biosampler to collect particulate matter for chemical analyses and gravimetric determination of the mass. The parallel filters are thus representative of the aerosol collected in the biosampler, and may be used to validate the representativeness of the chemical properties determined in view of toxicity assessments (Bessa *et al.*, 2020). Similar comparisons were carried out by Ning *et al.* (2006) and Saarikoski *et al.* (2014) for ambient aerosol, who concluded that for average concentrations ranging over four orders of magnitude (<ng/m^3 to 100s ng/m^3) very good agreements were found. In the present work this comparison was applied to indoor air aerosols, and at the opposite end of the concentration range (>1000 µg/m^3, Table 1).

Large similarities were observed between the relative particle chemical composition on the Teflon filters and in the biosampler (Fig. 6), which were especially remarkable for fine and UF particles (with the exception of fine particles in booth #1). Differences may have been expected with high contributions from water-soluble species, which was not the case as particles emitted during spraying were mainly metals and metal oxides. It should be remembered that fine and UF particles were collected directly from the inside of the spraying booths, while coarse particles were sampled from the worker area. This means that coarse particles were more influenced by indoor and outdoor background aerosols than fine and UF particles, and probably had a higher water-soluble content. As shown in Fig. 6, the relative composition of coarse particles sampled during spraying in both booths (but sampled in the worker area) showed certain differences between the Teflon and the biosampler samples which were, in any case, not large (e.g. Ca 31% versus 39% of the mass analysed in the biosampler versus Teflon samples, Al 20% versus 21%, or Fe 13% versus 14%). Finally, unexpected differences between the filter and biosampler composition were obtained for fine particles from booth #1, with higher relative contributions from Cr and Ni in the biosampler filters. This result could be due to technical issues such as lower particle collection efficiency during re-filling of the condensation water tanks during the collection of this sample, but it so far remains unexplained.

Aside from this discrepancy, our results evidence an overall good comparability between particle chemical composition on filters collected in parallel to and in the biosamplers in the VACES system, for concentrations in the range 1–1000 µg/m^3.

Summary and conclusions

An aerosol concentrator (VACES) was used to sample incidental ultrafine particles (UFPs), as well as fine ($PM_{2.5}$, including UFP) and coarse aerosols, simultaneously on filter substrates and in liquid to determine their physical–chemical properties in view of toxicological assessments. An industrial case study was selected with the aim to challenge the VACES system with high concentrations of UFPs and test its applicability in indoor industrial scenarios. Results supported the comparability of this tool with online monitors in terms of particle mass for UF, fine and coarse particles, for the high concentrations measured (up to 95 µg UFP/m^3). Similarly, our results evidence an overall good comparability between particle chemical composition on filters collected in parallel to and in the biosamplers in the VACES system, for concentrations in the range 1–1000 µg/m^3. While the large size of the instrument is challenging for deployment in industrial settings, this work evidences that representative results may be obtained as long as a sufficiently repetitive activity is monitored.

In this case study, UFP emission mechanisms and particle transformation in workplace air (vaporization of target metals and new particle formation) were assessed with a focus on particle chemistry. During thermal spraying, the spraying conditions (specifically, temperature) were a key driver of fractionation of metals (Ni, Cr) between UF and fine particle sizes. When spraying occurred at temperatures above the elemental vaporization point, the metals were found in the UF fraction as a result of new particle formation. Conversely, at lower spraying temperatures these potentially health-hazardous metals were found in coarser size fractions (fine and coarse). These mechanisms have evident health implications, as they determine the inhalation trajectory and deposition regions of ultrafine-sized Ni and Cr along the human respiratory tract. In addition to chemical properties, particle morphology (e.g. spherical coarse particles in booth #3 *vs*. irregular UFPs in booth #1) was a key element to understand particle formation mechanisms and their impact on exposure. For all size fractions, and especially for UFPs, these results evidence the need for a detailed understanding of incidental particle formation mechanisms due to their direct implications on particle composition and, thus, exposure. In

agreement with recent studies (Keyter *et al.*, 2019), it is advisable that the ultrafine size fraction (especially, incidental) should be included in personal exposure and risk assessments in occupational settings.

Acknowledgements

The authors kindly acknowledge TM COMAS (http://www.tmcomas.com) for their committed cooperation. The work was carried out in the framework of the CERASAFE project (www.cerasafe.eu).

Funding

This work was funded by SIINN ERA-NET (project id: 16), the Spanish MINECO (PCIN-2015-173-C02-01) and the French agency (Region Hauts de France). The Spanish Ministry of Science and Innovation (Project CEX2018-000794-S; Severo Ochoa) and the Generalitat de Catalunya (project number: AGAUR 2017 SGR41) provided support for the indirect costs for the Institute of Environmental Assessment and Water Research (IDAEA-CSIC). We acknowledge support of the publication fee by the CSIC Open Access Publication Support Initiative through its Unit of Information Resources for Research (URICI).

Authors' Contributions

M. Viana: Conceptualization, Formal analysis, Methodology, Writing – Original draft, review and editing, Supervision; A. Salmatonidis: Data curation, Formal Analysis, Writing - review and editing; S. Bezantakos: Methodology, Writing – review and editing; C. Ribalta: Data curation, Writing – review and editing; N. Moreno: Methodology, Data curation, Writing – review and editing; P. Córdoba: Methodology, Data curation, Writing – review and editing; F. Cassee: Methodology, Writing – review and editing; J. Boere: Methodology; S. Fraga: Conceptualization, Writing – review and editing; J.P Teixeira: Conceptualization; M.J. Bessa: Review and editing; E. Monfort: Writing – review and editing.

Conflict of Interest

The authors declare no conflict of interest.

References

Bessa MJ, Brandão F, Fokkens P *et al.* (2021) Toxicity assessment of industrial engineered and airborne process-generated nanoparticles in a 3D human airway epithelial in vitro model. *Nanotoxicology*; **15**: 542–57. doi:10.1080/17435390.2021.1897698.

Bessa MJ, Brandão F, Viana M *et al.* (2020) Nanoparticle exposure and hazard in the ceramic industry: an overview of potential sources, toxicity and health effects. *Environ Res*; **184**: 109297.

Billet S, Landkocz Y, Martin PJ *et al.* (2018) Chemical characterization of fine and ultrafine PM, direct and indirect genotoxicity of PM and their organic extracts on pulmonary cells. *J Environ Sci (China)*; **71**: 168–78.

Brouwer D, Berges M, Virji MA *et al.* (2012) Harmonization of measurement strategies for exposure to manufactured nano-objects; report of a workshop. *Ann Occup Hyg*; **56**: 1–9.

Burnett R, Chen H, Szyszkowicz M *et al.* (2018) Global estimates of mortality associated with longterm exposure to outdoor fine particulate matter. *Proc Natl Acad Sci USA*; **115**: 9592–7.

Byeon JH, Park JH, Hwang J. (2008) Spark generation of monometallic and bimetallic aerosol nanoparticles. *J Aerosol Sci*; **39**: 888–96.

Cohen AJ, Brauer M, Burnett R *et al.* (2017) Estimates and 25-year trends of the global burden of disease attributable to ambient air pollution: an analysis of data from the Global Burden of Diseases Study 2015. *Lancet*; **389**: 1907–18.

Corsini E, Vecchi R, Marabini L *et al.* (2017) The chemical composition of ultrafine particles and associated biological effects at an alpine town impacted by wood burning. *Sci Total Environ*; **587–588**: 223–31.

Curwin B, Bertke S. (2011) Exposure characterization of metal oxide nanoparticles in the workplace. *J Occup Environ Hyg*; **8**: 580–7.

Falk A, Schimpel C, Haase A *et al.* (2016) *Research roadmap for nanosafety. Part III: Closer to the market (CTTM)*. https://zenodo.org/record/1493492.

Fonseca AS, Maragkidou A, Viana M *et al.* (2015) Process-generated nanoparticles from ceramic tile sintering: emissions, exposure and environmental release. *Sci Total Environ*; **565**: 922–32.

Freney EJ, Heal MR, Donovan RJ *et al.* (2006) A single-particle characterization of a mobile Versatile Aerosol Concentration Enrichment System for exposure studies. *Part Fibre Toxicol*; **3**: 8.

Geller MD, Kim S, Misra C *et al.* (2002) A methodology for measuring size-dependent chemical composition of ultrafine particles. *Aerosol Sci Technol*; **36**: 748–62.

Gerlofs-Nijland ME, Bokkers BGH, Sachse H *et al.* (2019) Inhalation toxicity profiles of particulate matter: a comparison between brake wear with other sources of emission. *Inhal Toxicol*; **31**: 89–98.

Gonzalez-Pech NI, Stebounova LV, Ustunol IB *et al.* (2019) Size, composition, morphology, and health implications of airborne incidental metal-containing nanoparticles. *J Occup Environ Hyg*; **16**: 387–99.

Hämeri K, Lähde T, Hussein T *et al.* (2009) Facing the key workplace challenge: assessing and preventing exposure to nanoparticles at source. *Inhal Toxicol*; **21**: 17–24.

Hristozov D, Maccalman L, Jensen K *et al.* (2012) *Risk assessment of engineered nanomaterials*. *Nanotoxicology*; **6**: 880–98. doi:10.3109/17435390.2011.626534.

Keyter M, Van Der Merwe A, Franken A. (2019) Particle size and metal composition of gouging and lancing fumes. *J Occup Environ Hyg*; **16**: 643–55.

Kim S, Jaques PA, Chang M *et al*. (2001) Versatile concentration enrichment system (VACES) for simultaneous in vivo and in vitro evaluation of toxic effects of ultrafine, fine and course ambient particles. Part I: development and laboratory characterization. *J Aerosol Sci*; **32**: 1281–97.

Kuhlbusch TA, Asbach C, Fissan H *et al*. (2011) Nanoparticle exposure at nanotechnology workplaces: a review. *Part Fibre Toxicol*; **8**: 22.

Kuhlbusch TAJ, Wijnhoven SWP, Haase A. (2018) Nanomaterial exposures for worker, consumer and the general public. *NanoImpact*; **10**: 11–25.

Lelieveld J, Evans JS, Fnais M *et al*. (2015) The contribution of outdoor air pollution sources to premature mortality on a global scale. *Nature*; **525**: 367–71.

Liu D, Mariman R, Gerlofs-Nijland ME *et al*. (2019) Microbiome composition of airborne particulate matter from livestock farms and their effect on innate immune receptors and cells. *Sci Total Environ*; **688**: 1298–307.

Maynard AD, Aitken RJ. (2007) Assessing exposure to airborne nanomaterials: current abilities and future requirements. *Nanotoxicology*; **1**: 26–41.

Maynard AD, Baron PA, Foley M *et al*. (2004) Exposure to carbon nanotube material: aerosol release during the handling of unrefined single-walled carbon nanotube material. *J Toxicol Environ Health A*; **67**: 87–107.

Mendes L, Gini MI, Biskos G *et al*. (2018) Airborne ultrafine particles in a naturally ventilated metro station: Dominant sources and mixing state determined by particle size distribution and volatility measurements. *Environ Pollut*; **239**: 82–94.

Morawska L, Ayoko GA, Bae GN *et al*. (2017) Airborne particles in indoor environment of homes, schools, offices and aged care facilities: the main routes of exposure. *Environ Int*; **108**: 75–83.

Ning Z, Moore KF, Polidori A *et al*. (2006) Field validation of the new miniature versatile aerosol concentration enrichment system (mVACES). *Aerosol Sci Technol*; **40**: 1098–110.

Ntziachristos L, Ning Z, Geller MD *et al*. (2007) Fine, ultrafine and nanoparticle trace element compositions near a major freeway with a high heavy-duty diesel fraction. *Atmos Environ*; **41**: 5684–96.

Oberbek P, Kozikowski P, Czarnecka K *et al*. (2019) Inhalation exposure to various nanoparticles in work environment—contextual information and results of measurements. *J Nanoparticle Res*; **21**: 222.

Oberdörster G. (2001) Pulmonary effects of inhaled ultrafine particles. *Int Arch Occup Env Heal*; **74**: 1–8.

Oberdörster G, Stone V, Donaldson K. (2007) Toxicology of nanoparticles: a historical perspective. *Nanotoxicology*; **1**: 2–25.

Ozgen S, Becagli S, Bernardoni V *et al*. (2017) Analysis of the chemical composition of ultrafine particles from two domestic solid biomass fired room heaters under simulated real-world use. *Atmos Environ*; **150**: 87–97.

Perrone MG, Gualtieri M, Ferrero L *et al*. (2010) Seasonal variations in chemical composition and in vitro biological effects of fine PM from Milan. *Chemosphere*; **78**: 1368–77.

Pope CA 3rd, Coleman N, Pond ZA *et al*. (2019) Fine particulate air pollution and human mortality: 25+ years of cohort studies. *Environ Res*; **183**: 108924.

Querol X, Alastuey A, Rodriguez S *et al*. (2001) PM10 and PM2.5 source apportionment in the Barcelona Metropolitan area, Catalonia, Spain. *Atmos Environ*; **35**: 6407–19. doi:10.1016/S1352-2310(01)00361-2.

Querol X, Alastuey A, Viana MM *et al*. (2004) Speciation and origin of PM10 and PM2.5 in Spain. *J Aerosol Sci*; **35**: 1151–72.

Ribalta C, Koivisto AJ, López-Lilao A *et al*. (2019a) Testing the performance of one and two box models as tools for risk assessment of particle exposure during packing of inorganic fertilizer. *Sci Total Environ*; **650**(Pt 2): 2423–36.

Ribalta C, Koivisto AJ, Salmatonidis A *et al*. (2019b) Modeling of high nanoparticle exposure in an indoor industrial scenario with a one-box model. *Int J Environ Res Public Health*; **16**: 1695.

Saarikoski S, Carbone S, Cubison MJ *et al*. (2014) Evaluation of the performance of a particle concentrator for online instrumentation. *Atmos Meas Tech*; **7**: 2121–35.

Salmatonidis A, Ribalta C, Sanfélix V *et al*. (2019a) Workplace exposure to nanoparticles during thermal spraying of ceramic coatings. *Ann Work Expo Health*; **63**: 91–106.

Salmatonidis A, Sanfélix V, Carpio P *et al*. (2019b) Effectiveness of nanoparticle exposure mitigation measures in industrial settings. *Int J Hyg Environ Health*; **222**: 926–35.

Shao J, Wheeler AJ, Chen L *et al*. (2018) The pro-inflammatory effects of particulate matter on epithelial cells are associated with elemental composition. *Chemosphere*; **202**: 530–7.

Stone V, Miller MR, Clift MJD *et al*. (2017) Nanomaterials versus ambient ultrafine particles: an opportunity to exchange toxicology knowledge. *Environ Health Perspect*; **125**: 106002.

Terzano C, Di Stefano F, Conti V *et al*. (2010) Air pollution ultrafine particles: toxicity beyond the lung. *Eur Rev Med Pharmacol Sci*; **14**: 809–21.

Viana M, Fonseca AS, Querol X *et al*. (2017) Workplace exposure and release of ultrafine particles during atmospheric plasma spraying in the ceramic industry. *Sci Total Environ*; **599-600**: 2065–73.

Viana M, Rivas I, Querol X *et al*. (2014) Indoor/outdoor relationships and mass closure of quasi-ultrafine, accumulation and coarse particles in Barcelona schools. *Atmos Chem Phys*; **14**: 4459–72.

Viana M, Rivas I, Querol X *et al*. (2015) Partitioning of trace elements and metals between quasi-ultrafine, accumulation and coarse aerosols in indoor and outdoor air in schools. *Atmos Environ*; **106**: 392–401.

Viitanen AK, Uuksulainen S, Koivisto AJ *et al*. (2017) Workplace measurements of ultrafine particles-a literature review. *Ann Work Expo Health*; **61**: 749–58.